Communications in Physics, Vol. 33, No. 4 (2023), pp. 385-398
DOI: https://doi.org/10.15625/0868-3166/19168

Chaotic dynamics of a double-well Bose-Einstein condensate

Kalai Kumar Rajagopal† **and Cheng LongJun**

Department of Physics, Xiamen University Malaysia, Sepang 43900, Malaysia

E-mail: †kalaikumar.rajagopal@xmu.edu.my

Received 12 October 2023
Accepted for publication 28 November 2023
Published 12 December 2023

Abstract. *We study the dynamics of a double-well BEC system subjected to oscillating dissipation. The macroscopic model is described within the mean-field approximation while the noise effect due to large reservoir fluctuation has been averaged out to zero. We chose a simple dissipative memory kernel to produce a time-dependent oscillating dissipation. Our numerically calculated phase-space portraits and Lyapunov exponents show an enhanced route to chaos as one increases the driving dissipation amplitude.*

Keywords: double-well BEC; dissipation; quantum noise; Markovian; chaos.
Classification numbers: 03.75kk, 42.50Gg, 03.75Gg, 42.50Lc.

1. Introduction

The system of interacting Bose-Einstein Condensate (BEC) confined within a double-well out-coupled to reservoirs brings about many interesting quantum phenomena that have a close analogy with superconductor physics. Atom tunelling between the two wells induces phenomena such as population collapse and revival oscillations, see for instance the articles [1, 2].

Macroscopic quantum coherence is then established within the system. When stronger repulsive inter-particle interaction is present in the latter system, population imbalance oscillations get suppressed, and upon reaching a critical value, atoms start to localize forming what is known as the macroscopic quantum self-trapping state (MQST) [3,4]. Experimental measurement on thermal-induced phase fluctuations, Josephson's AC and DC effects, and interference fringe patterns on the double-well BEC system were the many fascinating features reported earlier by

©2023 Vietnam Academy of Science and Technology

experimental groups [5–9]. It became the stepping stone for further profound progress in the theoretical and experimental studies on the subject matter.

In an experimental setting, the system-environment condition requires one to consider classical instead of pure quantum physical reality. Dissipation and decoherence complicate the study. In particular, equilibrium phases of a double-well BEC systems diminish, leading towards complex non-linear dynamics, for instance, see in [10–17]. In contrast, Witthaut et. al. [13, 15] have shown that coherence could be sustained and enhanced under specific conditions. Their claim were supported then by the experimental findings reported in the articles [18, 19].

In general, the Markovian operational dynamics of a dissipative thermodynamic system is generated by $\delta-$ correlated memory kernel, whereas other type of memory kernels such as the Ornstein-Uhlenbeck (OU) [20] induces non-Markovian dynamics, for instance in [21–23]. We have applied extensively the latter type of memory kernels to study the Markovian (non-Markovian) dynamics of the double-well BEC reservoir systems [24–26].

In this work, we consider a system of double-well trap out-coupling to reservoirs in which the damping term is time-dependent. We introduced a generic time-dependent dissipative parameter which can be controlled by its amplitude and driving frequency. Implementing into the real experimental setup can be a challenging feat. We refer our model to the optical tweezer approach in [27, 28] modifying it into a generic double-well reservoir coupled system. The latter authors' models were inspired by the Wolfgang Ketterlee MIT groups' atom-laser experiment (Chikkatur et. al. [29]). In the latter experiment, each Bose-condensate is clamped by an optical tweezer and then brought closer to establish Bose-Josephson Junction (atoms are coherently coupled and may tunnel between the traps).

In the double-well BEC literature, the condition of small separation between the component is assumed so that BECs are coherently coupled establishing tunelling (condition for double-well BEC is satisfied). Modification on the optical tweezers employing pulsating lasers could provide an oscillation response on atoms in the double-well trap. We conceive that this may generate oscillating driving dissipation on the double well BEC-reservoir system. In parallel there are also studies on the time-dependent inter-particle interaction responses to the double-well BEC system, see for instance references in [30, 31]. Time-dependent inter-particle interaction is implemented by small frequency and amplitude oscillation of external field applied on the double-well barrier as reported in Saha et. al. [31]. A similar technique can also be employed to create an oscillating dissipation that transports atoms to reservoirs in a controllable manner.

The paper is organized as follows. The Hamiltonian of our double-well BEC-reservoir model is detailed in Sec. 2. The phase-space illustrating the system model is elaborated in Sec. 3. For clarity purposes, Sec. 3 is divided into two subsections describing (i) phase-space dynamics of constant dissipation and (ii) phase-space dynamics of the time-dependent dissipation. Lyapunov exponents which are quantitative measures of stability were tested in the latter subsection. Results are illustrated and discussed in brief. Finally, we conclude in Sec. 4.

2. Double-well BEC out-coupled to reservoirs

We consider a model of double-well atomic Bose-Einstein condensate (BEC) out-coupled to a reservoir at each trap (A and B). The full Hamiltonian of the system can be concisely described by

$$H_{Total} = H_{sys} + H_A + H_B + H_{sys-A} + H_{sys-B}. \tag{1}$$

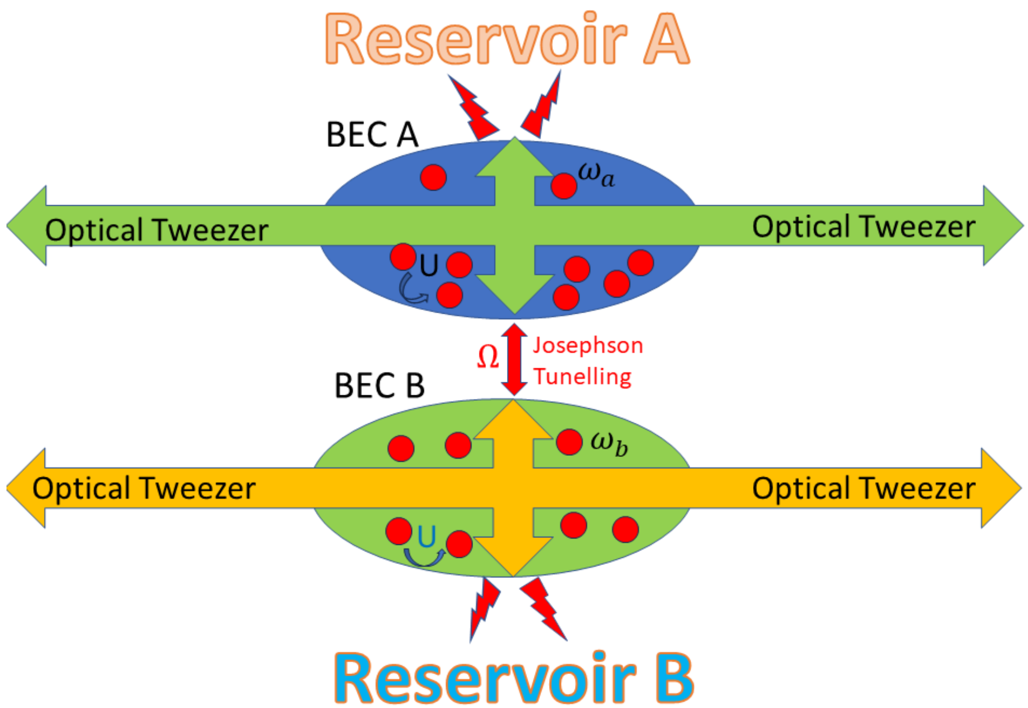

Fig. 1. Model of double-well BEC out-coupled to reservoirs.

The first term on the above equation represents a double-well loaded with Bose-Einstein condensate atoms which is then lucidly described by the following sub-Hamiltonian [2, 3, 14]:

$$H_{sys} = \hbar\omega_a \hat{a}^\dagger \hat{a} + \hbar\omega_b \hat{b}^\dagger \hat{b} + \hbar\Omega(\hat{a}^\dagger \hat{b} + \hat{b}^\dagger \hat{a}) + \frac{\hbar U}{2}(\hat{a}^\dagger \hat{a}^\dagger \hat{a}\hat{a} + \hat{b}^\dagger \hat{b}^\dagger \hat{b}\hat{b}), \tag{2}$$

where the first two terms describe free atoms (at each traps) with frequencies (ω_a, ω_b), $\hbar\Omega$ is the tunnelling splitting, U is the on-site inter-particle interaction strength. Sets $(\hat{a}^\dagger, \hat{a})$ and $(\hat{b}^\dagger, \hat{b})$ are the creation and annihilation operators of the boson at traps A and B, respectively.

Two separate reservoirs (or multi-mode fields) attached at each trap (A and B) are represented by $H_A = \sum_k \omega_k \hat{A}_k^\dagger \hat{A}_k$ and $H_B = \sum_k \omega_k \hat{B}_k^\dagger \hat{B}_k$. In this model, we assume reservoirs are composed of closely spaced oscillators with frequencies ω_k. Their corresponding creation and annihilation operators are $(\hat{A}_k^\dagger, \hat{A}_k)$ and $(\hat{B}_k^\dagger, \hat{B}_k)$, respectively. We suppose the reservoirs are in thermal equilibrium satisfying the following conditions:

$$\langle \hat{A}^\dagger(0)\rangle = \langle \hat{A}(0)\rangle = 0 \tag{3}$$

$$\langle \hat{B}^\dagger(0)\rangle = \langle \hat{B}(0)\rangle = 0 \tag{4}$$

$$\langle \hat{A}_k^\dagger(0)\hat{A}_{k'}(0)\rangle = \delta_{kk'} n_A(\omega_{k'}), \quad \langle \hat{B}_k^\dagger(0)\hat{B}_{k'}(0)\rangle = \delta_{kk'} n_B(\omega_{k'}) \tag{5}$$

$$\langle \hat{A}_k(0)\hat{A}_{k'}(0)\rangle = 0, \quad \langle \hat{B}_k(0)\hat{B}_{k'}(0)\rangle = 0 \tag{6}$$

where $n_j(\omega_k) = 1/[\exp(\omega_k/k_B T_j) - 1]$ for $j = A, B$ are the average boson numbers at reservoirs A and B whereas (T_A, T_B) are their corresponding temperatures. k_B denotes Boltzmann constant. We set $T_A = T_B = T$ to avoid the production of heat current between the traps. Lastly, the system-reservoir interactions are denoted by the following sub-Hamiltonians:

$$\begin{aligned} H_{sys-A} &= \sum_k g_k(\hat{a}\hat{A}_k^\dagger + \hat{a}^\dagger \hat{A}_k) \\ H_{sys-B} &= \sum_k f_k(\hat{b}\hat{B}_k^\dagger + \hat{b}^\dagger \hat{B}_k), \end{aligned} \tag{7}$$

where g_k or f_k are the bi-linear out-coupling function of traps A or B respectively. The dynamical property of this system can be studied by solving the Heisenberg equation of motion $\frac{d\hat{O}}{dt} = -\frac{i}{\hbar}[\hat{O}, \hat{H}_{Total}]$ as shown in the text-books [21,22]:

$$\frac{d\hat{a}}{dt} = -i\,\omega_a\hat{a} - i\Omega\hat{b} - iU(t)\hat{a}^\dagger\hat{a}\hat{a} + F_a(t) - \int_0^t dt' K(t-t')a(t') \tag{8}$$

$$\frac{d\hat{b}}{dt} = -i\,\omega_b\hat{b} - i\Omega\hat{a} - iU(t)\hat{b}^\dagger\hat{b}\hat{b} + F_b(t) - \int_0^t dt' M(t-t')b(t'), \tag{9}$$

where

- $F_A(t) = -i\sum_k g_k\hat{A}_k(0)\exp(-i\omega_k t)$ and $F_B(t) = -i\sum_k f_k\hat{B}_k(0)\exp(-i\omega_k t)$ are to the internal noise induced by the reservoir fluctuations.
- Last terms of the above equations correspond to dissipation with memory kernels $K(t) = \sum_k g_k^2 \exp(-i\omega_k t)$ and $M(t) = \sum_k f_k^2 \exp(-i\omega_k t)$.

The choice of spectral function $S(\omega) = D(\omega)[g(\omega)]^2$ determines the type of memory kernel $K(t) = \sum_k g_k^2 \exp(-i\omega_k(t)) \to \int_0^\infty d\omega S(\omega)\exp(-i\omega t)$. For example, flat spectrum (constant) results in a memory-less dissipation kernel $K(t) = constant \times \delta(t)$. Systems with flat spectral function $S(\omega) = constant$ characterize white noise and they exhibit Markovian operational dynamics. Lorentzian spectral function in the form $S(\omega) = 2c/[c^2 + \omega^2]$ with constant c produces the Ornstein-Uhlenbeck (OU) memory kernel $K(t) = constant \times \gamma\exp(-\gamma t)$. Parameter γ is the correlation memory time [21–23]. For $\gamma \to \infty$ one recovers memory-less delta correlated kernel. A system where $S(\omega) \approx 1/\omega^2$ induces coloured noise and exhibits non-Markovian operational dynamics. In this work, we have introduced time-dependent dissipative parameters $K(t-t') = Q_1(1 + F\cos(\Omega_D t'))\delta(t-t')$ and $M(t-t') = Q_2(1 + F\cos(\Omega_D t'))\delta(t-t')$, into the memory kernels of the Eqs. (8)-(9),where F and Ω_D denote the driving amplitude and frequency respectively. The standard time-independent memory-less kernels are simply $K(t-t') = Q_1\delta(t-t')$ and $M(t-t') = Q_2\delta(t-t')$ with (Q_1, Q_2) corresponding to constant dissipation strengths at traps A and B respectively. Applying the above-mentioned information and criteria into Eqs. (8)-(9), we simplify it to the following form (variables are still in operator form):

$$\frac{d\hat{a}}{dt} = (-i\,\omega_a - \Gamma_A(t))\hat{a} - i\Omega\hat{b} - iU\hat{a}^\dagger\hat{a}\hat{a} + F_A(t) \tag{10}$$

$$\frac{d\hat{b}}{dt} = (-i\,\omega_b - \Gamma_B(t))\hat{b} - i\Omega\hat{a} - iU\hat{b}^\dagger\hat{b}\hat{b} + F_B(t), \tag{11}$$

where $\Gamma_A(t) = Q_1(1 + F\cos(\Omega_D t))$ and $\Gamma_B(t) = Q_2(1 + F\cos(\Omega_D t))$.

3. Phase-space in the Mean-field limit

In general, there are no exact remedies for such non-linear operator equations Eqs. (10)-(11), but an approximate solution can always be obtained by averaging them and decorrelating higher-order correlation operator function into products of lower ones. In the present work, we decorrelate the third-order moment appearing on the right-hand side of Eqs. (10)-(11) by the relation $\langle \hat{C}^\dagger \hat{C}\hat{C}\rangle \approx \langle \hat{C}^\dagger\rangle\langle \hat{C}\rangle\langle \hat{C}\rangle$ where $C = \{a,b\}$. This approximation is valid in the macroscopic limit since the covariance vanishes as O(1/N) (where N is the total number of atoms of the system) if the many-part quantum state is close to pure BEC [32]. In other words, the macroscopic dynamics (system with a large number of atoms, $N \to \infty$) of the BECs is still valid and well described by the mean-field approximation [2–4, 14].

Defining $\alpha = \langle \hat{a}\rangle$, $\alpha^* = \langle \hat{a}^\dagger\rangle$, $\beta = \langle \hat{b}\rangle$ and $\beta^* = \langle \hat{b}^\dagger\rangle$ with $n(t) = |\alpha|^2 + |\beta|^2 = n_A(t) + n_B(t)$ denoting the total particle number at certain time t in the double-well. For large reservoir system, averages $\langle F_A(t)\rangle$ and $\langle F_B(t)\rangle$ vanishes but their two-point (time) correlations $\langle F_A^\dagger(t)F_A(t')\rangle$ and $\langle F_B^\dagger(t)F_B(t')\rangle$ are non-zero. However here we consider only the single moment average for noise, hence ruling out the two-point noise correlations that satisfy the fluctuation dissipation theorem for the existence of internal noise (discussed elsewhere, see for instance our earlier work [25]). In case there exist higher order moments, they can be decorrelated to a single moment again. With the said information, Eqs. (10)-(11), can be remodelled into the following mean-field equations:

$$\frac{d\alpha}{dt} = (-i\omega_a - \Gamma_A(t))\alpha - i\Omega\beta - iU|\alpha|^2\alpha\,, \tag{12}$$

$$\frac{d\beta}{dt} = (-i\omega_b - \Gamma_B(t))\beta - i\Omega\alpha - iU|\beta|^2\beta\,. \tag{13}$$

3.1. Dynamics of system subjected to constant dissipation

The dynamics of our system can be captured by the phase-space portrait $(z(t),\theta(t))$ where z(t) is the population imbalance between the traps and $\theta(t)$ is their phase-difference. For the phase-space representation we re-defined the complex variables (α, β) more precisely by $\alpha = |\alpha|\exp(i\theta_a)$ and $\beta = |\beta|\exp(i\theta_b)$. Population imbalance is defined by $z(t) = (|\alpha|^2 - |\beta|^2)/n(t)$ where $n(t) = (|\alpha|^2 + |\beta|^2)$ is the total number of atoms in the double-well, while the relative phase at any instance is $\theta(t) = \theta_a(t) - \theta_b(t)$. We set $\omega = \omega_a = \omega_b$ assuming a symmetric double-well trap.

Using the definition of $z(t)$ and $\theta(t)$ and performing some algebra on Eqs. (12)-(13), we obtain the following set of coupled dynamical equations [26, 33]:

$$\frac{dz}{dt} = -2\sqrt{1-z^2}\sin\theta + \eta(1-z^2)\,, \tag{14}$$

$$\frac{d\theta}{dt} = \frac{2z\cos\theta}{\sqrt{1-z^2}} - Uz\,. \tag{15}$$

The equations above are controlled by the dissipation bias parameter $\eta = Q_1 - Q_2$ and interparticle interaction U (time-independent). Time has been scaled in unit Ω. Fixed-points of the system can be obtained by setting $\dot{z}=0$, $\dot{\theta}=0$ which then yields the following result:

$$\sin\theta = \frac{\eta}{2}\sqrt{1-z^2}\,,$$
$$\cos\theta = \frac{U}{2}\sqrt{1-z^2}\,. \tag{16}$$

Solving the above set of equations we obtain fixed points (z_*,θ_*)= { $(0,\theta_1)$, $(0,\pi-\theta_1)$, $(\pm m_o\,,\pi-\theta_2)$ } where $m_o=\sqrt{1-\frac{4}{U^2+\eta^2}}$, $\theta_1=\arcsin(U/2)$ and $\theta_2=\arccos(\frac{U}{\sqrt{\eta^2+U^2}})$. For the non-dissipative case ($\eta=0$), we change m_o to $s_o=\sqrt{1-\frac{4}{U^2}}$. Notice that the fixed-points are a function of inter-particle interaction and damping constant. Based upon the above Eqs. (14)–(15), Jacobian matrix can be derived in the following way:

$$\begin{aligned} M &= \begin{pmatrix} \frac{\partial\dot{z}}{\partial z} & \frac{\partial\dot{z}}{\partial\theta} \\ \frac{\partial\dot{\theta}}{\partial z} & \frac{\partial\dot{\theta}}{\partial\theta} \end{pmatrix} \\ &= \begin{pmatrix} 2z\sin\theta/\sqrt{1-z^2}-2\eta z & -2\sqrt{1-z^2}\cos\theta \\ -U+2\cos\theta/[1-z^2]^{3/2} & -2z\sin\theta/\sqrt{1-z^2} \end{pmatrix}. \end{aligned} \tag{17}$$

The Jacobian matrix above is evaluated at fixed-points (z_*,θ_*), and the eigenvalues describe its stability characteristics. The latter is based upon the following criteria which reads [34, 35]:

- two imaginary eigenvalues correspond to the formation of elliptic fixed-point,
- two real eigenvalues indicate the formation of hyperbolic fixed-point,
- two real eigenvalues with opposite sign indicate a saddle point,
- complex eigenvalue with negative real part represents an attractor,
- complex eigenvalue with positive real part represents a repeller.

Table 1 details the eigenvalues, trace and determinant for the non-dissipative and dissipative cases.

3.2. Dynamics of system subjected to time-dependent dissipation

For the driven time-dependent dissipation, the phase-space portrait is expanded to three dimensions defined by the vector $Z=(z(t),\ \theta(t),\ \phi(\mathrm{t}))$. Again, the equilibrium or fixed-points are determined by setting $\dot{Z}=0$. Periodically varying the dissipation might drive the system to an equilibrium (fixed-points) or non-periodic (chaotic) state. That needs to be determined now. We reformulate Eqs. (14) and (15) incorporating the time-dependent dissipation term. The new dynamical equations are:

$$\frac{dz}{dt} = -2\sqrt{1-z^2}\,\sin\theta+\zeta(t)(1-z^2)\,, \tag{18}$$
$$\frac{d\theta}{dt} = \frac{2z\cos\theta}{\sqrt{1-z^2}}-U\,z\,, \tag{19}$$
$$\frac{d\phi}{dt} = \Omega_D\,. \tag{20}$$

Here $\zeta(t)=\Gamma_A(t)-\Gamma_B(t)=\eta(1+F\cos\phi)$ is the time-dependant dissipation parameter with bias η already defined earlier. We have introduced parameter $\phi=\Omega_D t$ to transform the non-autonomous ordinary differential equation (ODE) in the form $\dot{X}=(\dot{z}(t),\dot{\theta}(t))'=F(z(t),\theta(t),t)$

Table 1. Eigenvalues, trace and determinant of the Jacobian matrix (17) for the system with and without dissipation. On each cell, the first line corresponds to Jacobian eigenvalues, the second line is represented by the symbol (p,sign), where p is trace of the Jacobian matrix or addition of eigenvalues which is a real or complex number whereas the sign indicates whether its determinant is > 0, < 0 or simply zero. The third line denotes the characteristic of fixed-points.

Non-dissipative η=0	U=0.1	U=1.0	U=2.0	U=2.5
M(0,0)	±1.95i (0,+) elliptic	±1.41 (0, +) elliptic	0,0 (0, 0)	±1 (0, -) saddle
M(0,π)	±2.05i (0,+) elliptic	±2.45i (0,+) elliptic	±2.83i (0,+) elliptic	±3i (0,+) elliptic
M(s_o,π)			±2.83i (0,+) elliptic	±1.5i (0,+) elliptic
M($-s_o$,π)			±2.83i (0,+) elliptic	±3.2i (0,+) elliptic
Dissipative $\eta = 0.1$				
M$(0,\theta_1)$	±1.95i (0,+) elliptic	±1.41i (0,+) elliptic	0,0 (0,0)	±1 (0,-) saddle
M$(0,\pi-\theta_1)$	±2.05i (0,+) elliptic	±2.45i (0,+) elliptic	±2.81i (0,+) elliptic	±3i (0,+) elliptic
M$(m_o,\pi-\theta_2)$			-0.01±2.83i (-0.01,+) attractor	-0.06±3.20i (-0.12,+) attractor
M$(-m_o,\pi-\theta_2)$			0.01±2.83i (0.01,+) repeller	0.06±3.20i (-0.12,+) repeller

to an autonomous ODE $\dot{X} = (\dot{z}(t), \dot{\theta}(t), \dot{\phi}(t))' = G(z, \theta, \phi)$. Evolution of phase diagrams (z,θ,ϕ) governed by the main control parameters (U, η, F, Ω_D) are plotted in Figs. 3 and 4. The focus of this work is to study the dynamics closer to the onset of chaos, or when equilibrium states such as the macroscopic quantum coherence (occur at weak interaction) or localized MQST perturbed [24, 26, 33].

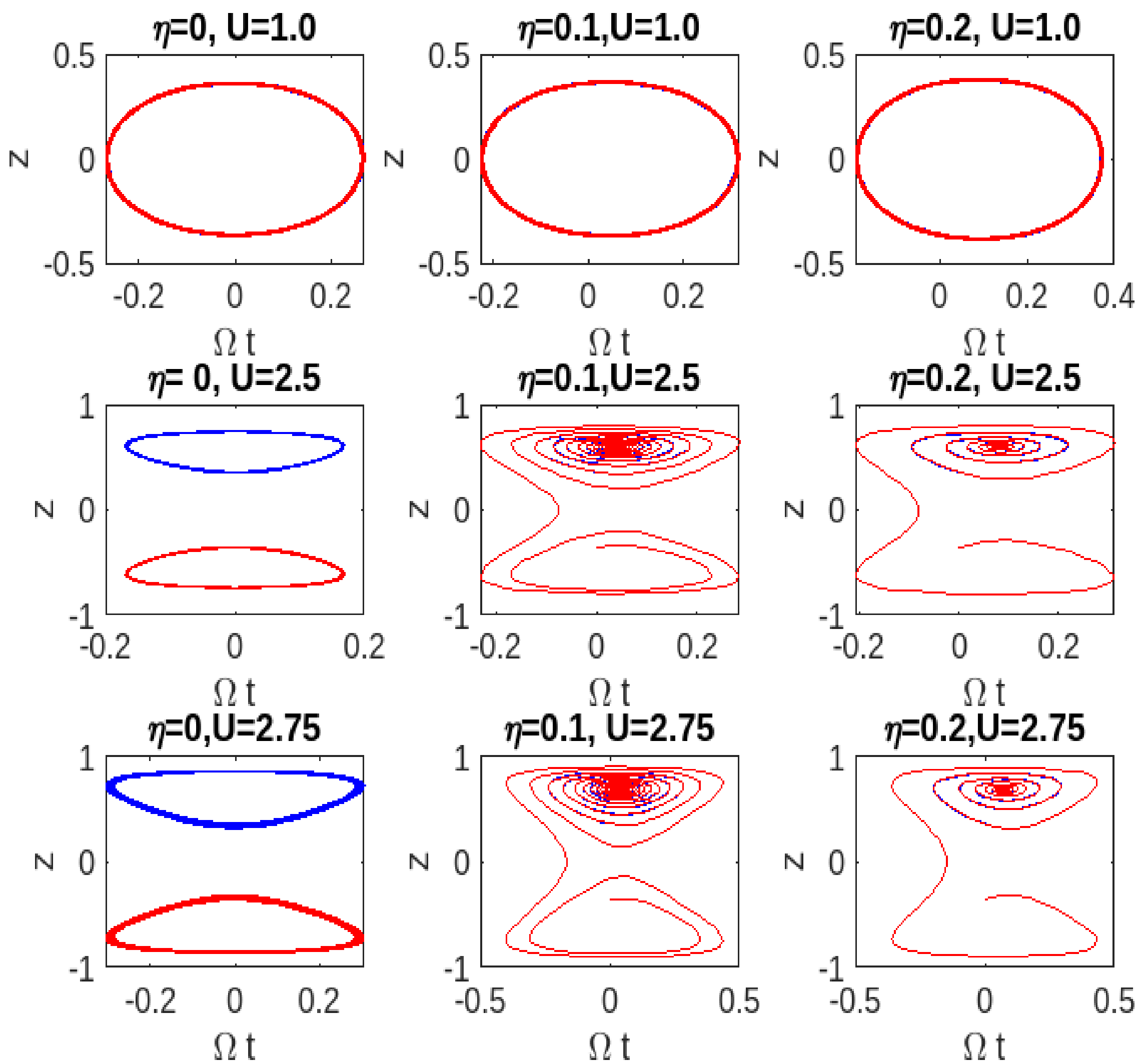

Fig. 2. Phase space (z,θ) evolution of the BEC system as a function of inter-particle interaction strength U and dissipation strength η. Initial conditions are ($z(0)$, $\theta(0)$)=($\pm0.64, 0$) while the trajectories run for t=300. Phases are evolving from Quantum Tunelling state (QTS) (elliptic trajectories) at $U = 1.0$ to Macroscopic Quantum Self-trapping (hyperbolic trajectories) $U = \{2.5, 2.75\}$. Phase difference θ is plotted in unit radian.

We have seen in the previous sub-section that the phase-space diagram illustrates qualitatively the complex non-linear dynamics of the system at critical points featuring fixed-points and attractors. However, Lyapunov characteristics exponents (LCE) provide a precise quantitative convergence or divergence measure of the generated close-by trajectories [35]. We numerically compute the LCEs employing the Benettin algorithm, details of which can be found in the reference [36].

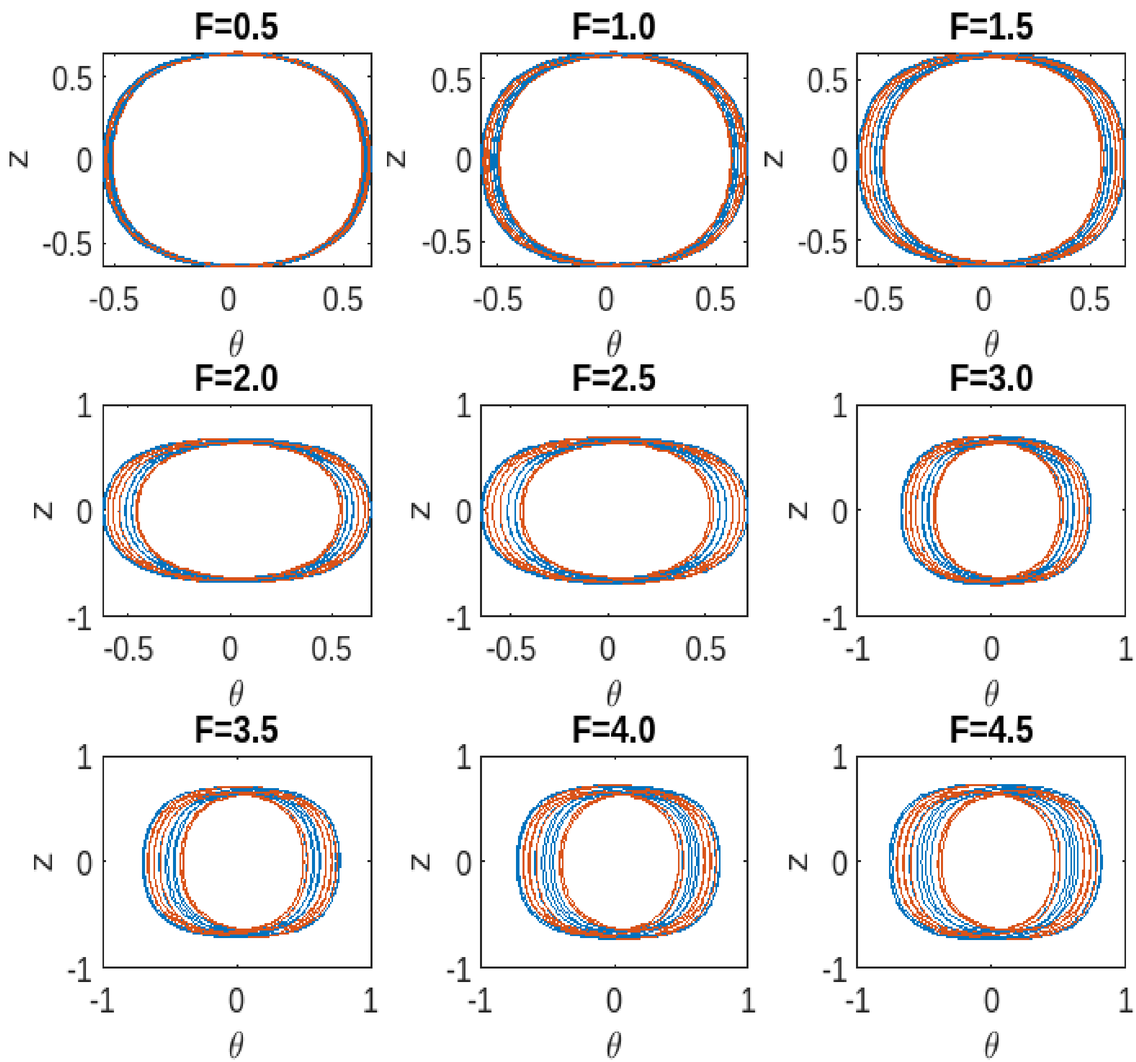

Fig. 3. Phase space evolution on the plane (z,θ) for the system driven by dissipation as a function of driving amplitude F. Driving frequency is fixed at $\Omega_D = \pi/6$ at weak inter-particle interaction with strength $U = 0.75$. Initial conditions are ($z(0)$, $\theta(0)$,$\phi(0)$)=($\pm 0.64, 0, 0$) while the trajectories runs for t=300. Phase difference θ, is plotted in unit radian.

Usually, the Lyapunov exponent or Lyapunov characteristic exponent of a dynamical system is a quantity that characterizes the rate of infinitesimal separation of close trajectories Z(t) and $Z_0(t)$ in phase space. Let $\delta Z(t) = Z(t) - Z_o(t)$ and $\delta Z_o = Z(0) - Z_o(0)$, if $|\delta Z(t)| \approx \exp(\lambda t)|\delta Z_o|$ then λ is treated as the Lyapunov exponent. If the trajectory Z(t) is given by an n-dimensional linear ordinary differential equation system with constant coefficients $\dot{Z} = \mathbf{A}Z + \mathbf{F}(t)$. For a dynamical system with evolution equation $\mathbf{F}(t)$ in n-dimensional phase space, the spectrum of Lyapunov exponents $\lambda_1, \lambda_2, \ldots, \lambda_n$, in general, depends on the initial point x_o. The Lyapunov exponents

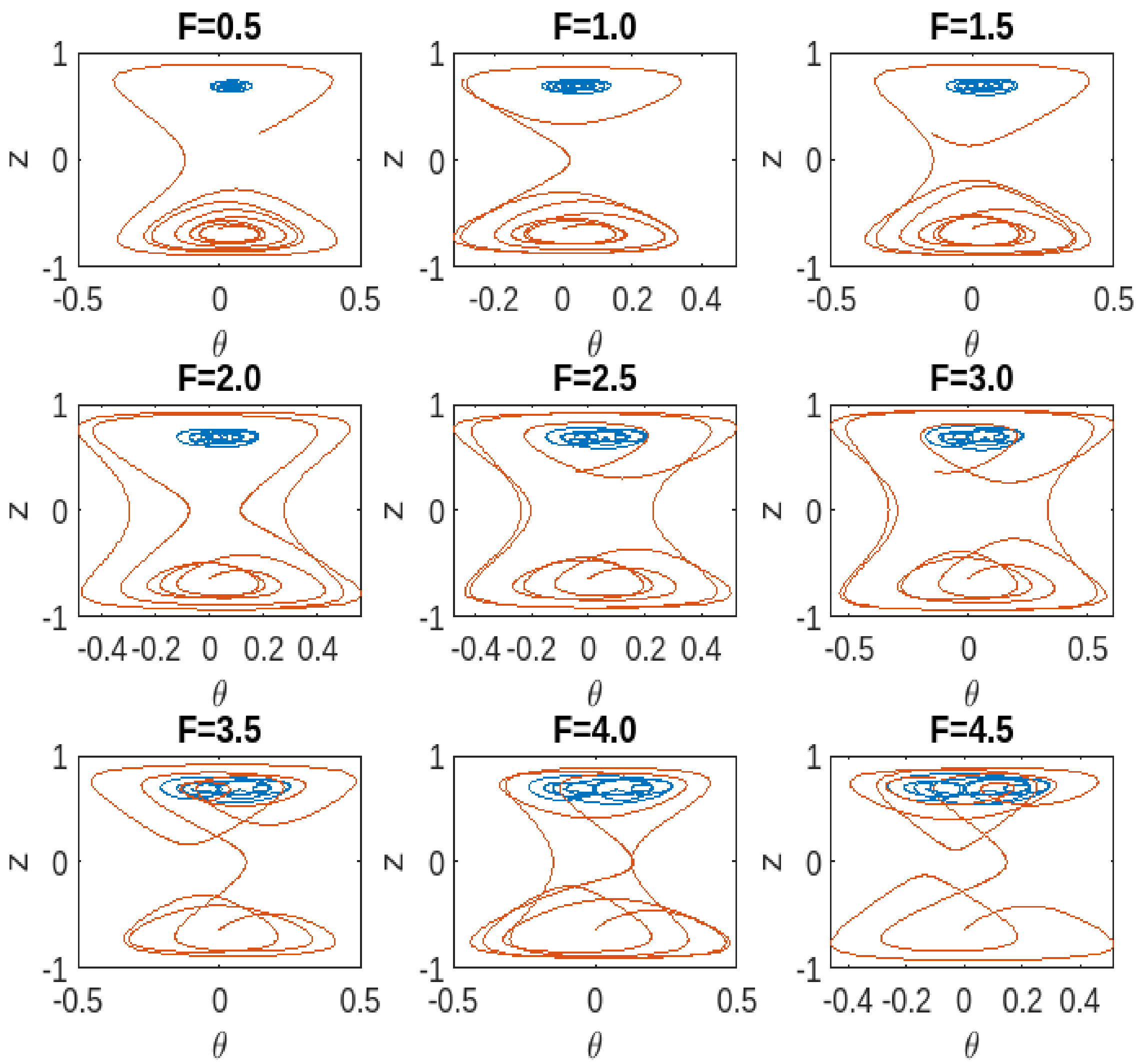

Fig. 4. Same as in Fig. 3 but for U = 2.75.

describe the behaviour of vectors in the tangent space of the phase space and defined from the Jacobian matrix $J_{ij}(t) = \frac{f_i(t)}{dx_i}|_{x_o}$ (matrix $\mathbf{J}$ whose elements evaluated at initial value x_o) while f_i is the element of vector $\mathbf{F}$. Then the evolution of small increment $\delta Z = (\delta z(t), \delta\theta(t), \delta\phi)'$ culminated from linearized solution of the equation $\delta\dot{Z}(t) = \mathbf{J}(x_o)\cdot\delta Z(t)$. The real parts of the n-different eigenvalue of the Jacobian matrix $\mathbf{J}$ is naturally the Lyapunov exponents, where the largest value of them is defined by [36, 37]:

$$\lambda_{max}(t) = \lim_{t\to\infty} \lim_{|\delta Z_o(t)|\to 0} \frac{1}{t} \ln \frac{|\delta Z(t)|}{|\delta Z_o(t)|}. \tag{21}$$

We follow criterion in reference [37] (see also text-books on dynamical systems and chaos such as [35, 38–40]) which states that the system attractors reduce to (i) stable fixed points, if all the Lyapunov exponents are negative, (ii) a limit cycle if one Lyapunov exponent is zero and the remaining exponents are all negative, (iii) k-dimensional torus if the first k Lyapunov exponents vanish while the remaining ones are negative and (iv) a strange attractor which is chaotic if at least one Lyapunov exponent is positive. Table 2 below summarizes the criterion stated above.

Table 2. Types of attractors based on the set of Lyapunov exponents for three-dimensional phase space.

Types of attractors	Signs of LCEs (λ_1,λ_2,λ_3)
Fixed-point	(-, -, -)
Limit cycle	(-, -, 0)
Torus T^2	(-, 0, 0)
Strange attractor	(-, 0, +)

Table 3 below depicts the steady-state Lyapunov exponents yielded by our simulation:

Table 3. Lyapunov exponents and Kaplan-Yorke dimension for given parameters.

Inter-particle interaction strength	Driving parameters	LCE λ_1	LCE λ_2	LCE λ_3	DKY
U=0.75	F=1.8, $\Omega_D = \pi/6$	-0.015	-0.003	0	1
U=0.75	F=1.9, $\Omega_D = \pi/6$	0.0164	-0.031	0	2.529
U=2.75	F=4.25, $\Omega_D = \pi/6$	-0.007	-0.141	0	1
U=2.75	F=4.5, $\Omega_D = \pi/6$	0.047	-0.198	0	2.237

Ordering the LCEs in such a way that $\lambda_1 > \lambda_2 ... > \lambda_j$ where j is the largest integer such that $\lambda_1 + \lambda_2 + ... + \lambda_j \geq 0$ accordingly, one can find the Kaplan-Yorke dimension (DKY) as following [36]:

$$DKY = j + \frac{\sum_{i=1}^{j} \lambda_j}{|\lambda_{j+1}|} \tag{22}$$

Fractional Kaplan-Yorke dimensions on Table 3 recognize non-periodic (or chaotic) solution for the larger driving amplitudes F in both weakly and strongly interacting system. Please note that we have depicted only parameters around the onset of chaos and their Lyapunov characteristics exponents (LCE) are computed numerically and depicted in Fig. 5.

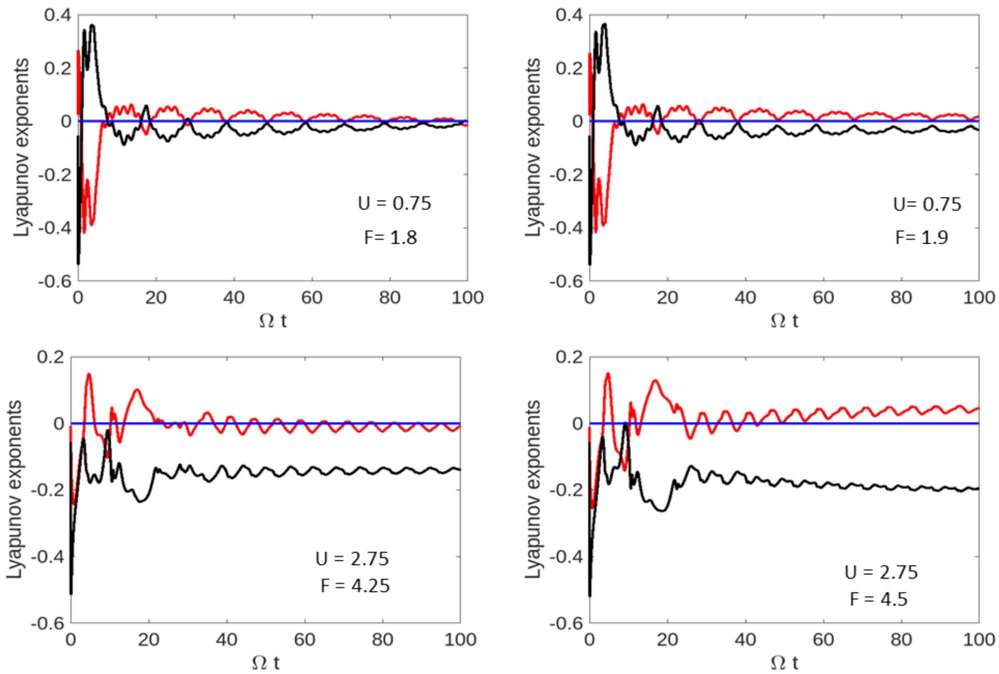

Fig. 5. Lyapunov exponent evolution of our system as a function of dissipation with amplitude F and driving frequency fixed at $\Omega_D = \pi/6$. The dissipation strength bias between the two wells is set at $\eta = 0.1$. The top panel is for weak on-site inter-particle interaction with strength $U = 0.75$, while the bottom panels are for $U = 2.75$. Dynamics of the system is generated by an initial condition $(z(0), \theta(0), \phi(0)) = (0.64, 0, 0)$.

4. Conclusions

We have analysed the complex non-linear dynamics of the double-well BEC system subjected to time-dependent dissipation. The operational dynamics is Markovian and the macroscopic system is valid within the Mean-field approximation. We extensively use the Matlab 0DE-45 solver in solving the system of first order non-linear ODE equation that arises from our model. Converging results can only be obtained using small parameter values. ODE-45 solver is a MATLAB numerical tool that employs an build-in Runge-Kutta fourth-order (RK4) algorithm. The mentioned solver is reliable in solving non-stiff ordinary or non-linear differential equations such as Van der Pol or Duffing equations.

In the double-well BEC literature, one sees elliptic trajectories around its fixed points which appear at weak inter-particle interaction indicating the Quantum coherence phase. On the other hand, MQST is depicted by hyperbolic trajectories around its fixed points present at stronger inter-particle interaction. In this work, we have chosen the mentioned two distinctive inter-particle interaction regimes to study the effect when the system is driven by time-dependent dissipation. The system's dynamics are controlled by the competition between inter-particle interaction and dissipation which itself is a function of amplitude and frequency. We have found that increasing driving amplitudes enhances systems' route to chaos. A large amplitude is needed for this transition at a stronger interacting regime.

The limitation of this work is that it uses only simple dissipation, culminating from the delta-correlated memory kernel. The internal noise has been averaged out (by the single moment average) though the noise-noise correlation is not negligible for which the system obeys the Fluctuation-dissipation theorem. However, dissipation still prevails in the system. Mean-field approximation requires only single moment averages, hence complicated two-point correlations of particles or noises have been neglected for simplicity. Including them results in a beyond mean-field approach which was reported by one of us in our earlier study of the system subjected to constant dissipation. We may consider it in future work.

Acknowledgments

We thank the examiners for their careful review and comments on this article.

Authors contributions

K. K. R.: Methodology, investigation, analysis and supervision. C.L.J: Literature survey and computation.

Conflict of interest

The authors have no conflict of interest to declare. They also declare that they have no competing financial interests.

References

[1] J. Javanainen, *Oscillatory exchange of atoms between traps containing bose condensates*, Phys. Rev. Lett. **57** (1986) 3164.

[2] G. Milburn, J. Corney, E. Wright and D. Walls, *Quantum dynamics of an atomic bose-einstein condensate in a double-well potential*, Phys. Rev. A **55** (1997) 4318.

[3] A. Smerzi, S. Fantoni, S. Giovanazzi and S. Shenoy, *Quantum coherent atomic tunneling between two trapped bose-einstein condensates*, Phys. Rev. Lett. **79** (1997) 4950.

[4] S. Raghavan, A. Smerzi, S. Fantoni and S. Shenoy, *Coherent oscillations between two weakly coupled bose-einstein condensates: Josephson effects, π oscillations, and macroscopic quantum self-trapping*, Phys. Rev. A **59** (1999) 620.

[5] M. Albiez, R. Gati, J. Fölling, S. Hunsmann, M. Cristiani and M. K. Oberthaler, *Direct observation of tunneling and nonlinear self-trapping in a single bosonic josephson junction*, Phys. Rev. Lett. **95** (2005) 010402.

[6] R. Gati, B. Hemmerling, J. Fölling, M. Albiez and M. K. Oberthaler, *Noise thermometry with two weakly coupled bose-einstein condensates*, Phys. Rev. Lett. **96** (2006) 130404.

[7] T. Zibold, E. Nicklas, C. Gross and M. K. Oberthaler, *Classical bifurcation at the transition from rabi to josephson dynamics*, Phys. Rev. Lett. **105** (2010) 204101.

[8] S. Levy, E. Lahoud, I. Shomroni and J. Steinhauer, *The ac and dc josephson effects in a bose–einstein condensate*, Nature **449** (2007) 579.

[9] S. Hofferberth, I. Lesanovsky, T. Schumm, A. Imambekov, V. Gritsev, E. Demler *et al.*, *Probing quantum and thermal noise in an interacting many-body system*, Nature Physics **4** (2008) 489.

[10] J. Ruostekoski and D. F. Walls, *Bose-einstein condensate in a double-well potential as an open quantum system*, Phys. Rev. A **58** (1998) R50.

[11] Y. Khodorkovsky, G. Kurizki and A. Vardi, *Bosonic amplification of noise-induced suppression of phase diffusion*, Phys. Rev. Lett. **100** (2008) 220403.

[12] E. Boukobza, M. Chuchem, D. Cohen and A. Vardi, *Phase-diffusion dynamics in weakly coupled bose-einstein condensates*, Phys. Rev. Lett. **102** (2009) 180403.

[13] D. Witthaut, F. Trimborn and S. Wimberger, *Dissipation induced coherence of a two-mode bose-einstein condensate*, Phys. Rev. Lett. **101** (2008) 200402.

[14] F. Trimborn, D. Witthaut and S. Wimberger, *Mean-field dynamics of a two-mode bose–einstein condensate subject to noise and dissipation*, J. Phys. B **41** (2008) 171001.

[15] D. Witthaut, F. Trimborn and S. Wimberger, *Dissipation-induced coherence and stochastic resonance of an open two-mode bose-einstein condensate*, Phys. Rev. A **79** (2009) 033621.

[16] Y. Huang, Q.-S. Tan, L.-B. Fu and X. Wang, *Coherence dynamics of a two-mode bose-einstein condensate coupled with the environment*, Phys. Rev. A **88** (2013) 063642.

[17] E. Ghasemian and M. Tavassoly, *Quantum dynamics of a bec interacting with a single-mode quantized field under the influence of a dissipation process: thermal and squeezed vacuum reservoirs*, Laser Physics **27** (2017) 095202.

[18] V. Guarrera, P. Würtz, A. Ewerbeck, A. Vogler, G. Barontini and H. Ott, *Observation of local temporal correlations in trapped quantum gases*, Phys. Rev. Lett. **107** (2011) 160403.

[19] G. Barontini, R. Labouvie, F. Stubenrauch, A. Vogler, V. Guarrera and H. Ott, *Controlling the dynamics of an open many-body quantum system with localized dissipation*, Phys. Rev. Lett. **110** (2013) 035302.

[20] G. E. Uhlenbeck and L. Ornstein, *On the theory of the brownian motion*, Physical Review **36** (1930) 823.

[21] U. Weiss, *Quantum dissipative systems*, vol. 10. World Scientific, 1999.

[22] M. Scully and M. Zubairy, *Quantum Optics*. Cambridge University Press, 1997.

[23] Y. Yamamoto and A. Imamoglu, *Mesoscopic quantum optics*. John Wiley & Sons, Inc., New York, 1999.

[24] K. K. Rajagopal and G. Ibragimov, *Non-linear dynamics of a double-well bose-einstein condensate-reservoirs system*, Braz. J. Phys. **50** (2020) 178.

[25] K. K. Rajagopal and G. Ibragimov, *Non-equilibrium yynamics of a double-well bose-einstein condensate-dual reservoirs system*, Braz. J. Phys. **51** (2021) 944.

[26] K. K. Rajagopal, G. Ibragimov, R. M. Hasim and I. A. Alias, *Jordan j. phys.*, Jordan Journal of Physics **15** (2022) 445.

[27] C. Lazarou, G. Nikolopoulos and P. Lambropoulos, *Non-markovian dynamics in atom-laser outcoupling from a double-well bose–einstein condensate*, J. Phys. B **40** (2007) 2511.

[28] G. Nikolopoulos, C. Lazarou and P. Lambropoulos, *Effects of relative phase and interactions on atom-laser outcoupling from a double-well bose–einstein condensate: Markovian and non-markovian dynamics*, J. Phys. B **41** (2008) 025301.

[29] A. Chikkatur, Y. Shin, A. Leanhardt, D. Kielpinski, E. Tsikata, T. Gustavson *et al.*, *A continuous source of bose-einstein condensed atoms*, Science **296** (2002) 2193.

[30] F. K. Abdullaev, J. Shaari and M. Wahiddin, *Coupled-mode theory for bose–einstein condensates with time dependent atomic scattering length*, Phys. Lett. A **345** (2005) 237.

[31] A. K. Saha, D. S. Ray and B. Deb, *Parametric oscillations in a dissipative bosonic josephson junction*, J. Phys. B **53** (2020) 135301.

[32] F. Trimborn, D. Witthaut and H. Korsch, *Beyond mean-field dynamics of small bose-hubbard systems based on the number-conserving phase-space approach*, Phys. Rev. A **79** (2009) 013608.

[33] C. Bo, W. Song-Lin and Y. Xue-Xi, *Mean-field dynamics of a two-mode bose-einstein condensate subject to decoherence*, Chin. Phys. Lett. **27** (2010) 070303.

[34] L. Perko, *Differential equations and dynamical systems*, vol. 7. Springer Science & Business Media, 2013.

[35] S. H. Strogatz, *Nonlinear dynamics and chaos with student solutions manual: With applications to physics, biology, chemistry, and engineering*. CRC press, 2018.

[36] M. Sandri, *Numerical calculation of lyapunov exponents*, Math. J. **6** (1996) 78.

[37] D. H. Rothman, *Nonlinear dynamics I: Chaos*, Massachussetts Institute of Technology, 2012.

[38] G. M. Zaslavsky, *The physics of chaos in Hamiltonian systems*. World Scientific, 2007.

[39] M. Lakshmanan and S. Rajaseekar, *Nonlinear dynamics: integrability, chaos and patterns*. Springer Science & Business Media, 2012.

[40] R. L. Devaney and K. T. Alligood, *Chaos and fractals: The mathematics behind the computer graphics: The mathematics behind the computer graphics*, vol. 1. American Mathematical Soc., 1989.